Impact of the N-glycosylation on full-length IgG2 and IgG4 antibodies: a comparative study using molecular dynamics simulations.

Ravy Leon Foun Lin, Adam Bellaiche, Julien Diharce and Catherine Etchebest

Abstract: Like other proteins, monoclonal antibodies - important biodrugs- are subject to post translational modifications, especially the N-glycosylations. However, the effect of the N-glycosylations remains poorly studied and atomistic details about their influence are rarely available. . Moreover, the few existing studies focus on the prevalent immunoglobulin G1. To go further in the understanding of the impact of glycosylations, we have carried out a comparative exploration of the effect of N-glycosylations on two different classes of antibodies, namely Mab231, an IgG2 and the pembrolizumab, an IgG4 . The two antibodies differ by their sequences, their length, their 3D structure but also by the location and composition of the glycans. In the present work, detailed and important information were gained through molecular dynamics simulations where both monoclonal antibodies were studied without and with the presence of their glycans. The results of 1.5 µs of sampling for each system show that glycosylation does not drastically alter the overall conformational landscape of either antibody, whatever the metrics considered. However, it measurably modulates local flexibility, inter-domain correlated motions, and the relative orientation of the Fab arms with respect to the Fc domain, with statistically significant shifts in key geometric descriptors. Importantly, contact analysis reveals that glycan interactions extend beyond the Fc region to reach Fab residues. The allosteric network calculations demonstrate that the influence of Fc-bound glycans propagates even until the Fab framework regions in both mAbs, which could impact the antigen binding. The nature and magnitude of these effects are subclass-dependent, reflecting differences in glycan composition, hinge architecture, and three-dimensional organization Our findings challenge the prevailing view that Fc glycosylation uniformly promotes CH2 domain opening. More importantly, it underscores the necessity of considering full-length structures and IgG subclass diversity in glyco-engineering strategies.

INTRODUCTION.

Monoclonal antibodies (mAbs) are proteins part of the immunoglobulin G (IgG) class[1] . They are mainly used in the pharmaceutical[2–4] industry and in the biotechnology[5,6] field, i.e. in cancer[2,6–8] and leukaemia treatment[9–12], or for diagnostics purposes through several usual biological tests such as the ELISA test[13]. Their ability to specifically bind, via their complementarity-determining regions (CDR), to a unique target[5] is a major advantage for minimizing undesired immune responses, as well for detecting and neutralizing specific pathogens. However, polyspecificity, cross-reactivity, limited stability or low binding affinity are also observed in some mAbs cases, which compromise the host defense. Consequently, designing new antibodies with improved

specificity, higher affinity and enhanced stability is still a key objective pursued by biotechnology and pharmaceutical companies[1]. Various *in vitro*, *in silico* and *in vivo* methods and protocols have been developed to design mAbs, particularly through the optimization of their CDRs, to recognize specific targets[14–16]. For example, these approaches can also help to stabilize the mAb structure or to improve their binding specificity to proteins present within a mixture containing other molecules[1,9,13,17]. Although the functional properties are now well characterized[4,6,18,19], the full-length structure of IgG dynamics remains poorly studied[20]. IgGs are composed of three mains fragments named: Fc for Fragment crystallizable (Fc) and two Fabs for Fragments antigen binding[19,21,22] (Fig. 1). The Fabs are composed of a light chain and a heavy chain and contain at their top the CDRs involved in the antigens recognition[19]. These chains are connected by several disulfide bonds[21]. On the other hand, the Fc region interacts with Fc receptors that can be found on a cell surface[23,24], or can fix the cellular effectors[25–27], for example. It is constituted by two heavy chains, also connected by several disulfide bonds. These domains (Fc and two Fabs), composed of several immunoglobulin folds (rich in β-sheets) are joined by a disordered region called the Hinge. This highly flexible region[14] also comprises two heavy chains, linked by disulfide bonds[21] (Fig. 1). Those particularities and those three kinds of domains, make the full length-structures difficult to resolve using experimental methods like X-ray crystallography[21]. Owing to their smaller size and reduced flexibility, the individual structures of the Fc and Fab domains have been more readily determined[28] and numerous three-dimensional structures have been deposited on the Protein Data Bank[29,30] (PDB). In contrast, only a few full length structures, that encompass the Fab and Fc domains, are available at varying ranges of resolution (e.g: 5DK3 2.28 Å, 1IGT 2.80 Å , 1MCO 3.20 Å).

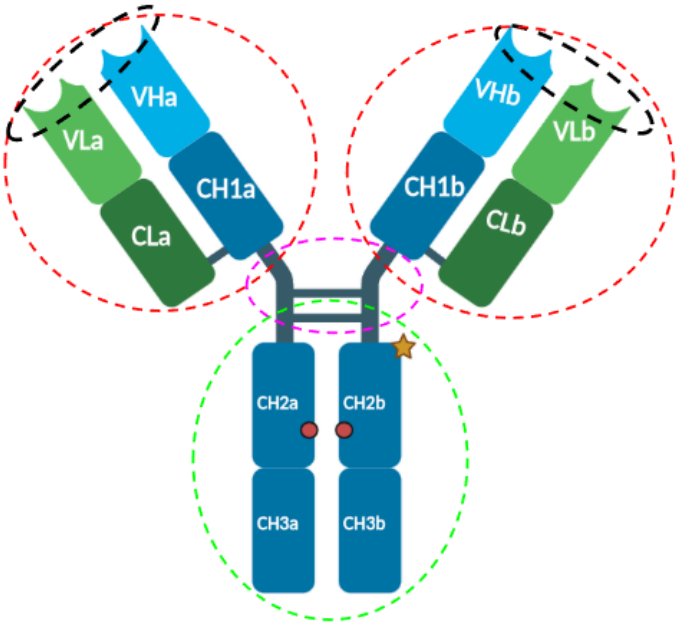

Figure 1: Schematic representation of a full length IgG. The blue regions are the heavy chains. The green regions are the light chains. The green dotted circle represents the Fc region. The pink dotted circle surrounds the hinge region. The red dotted circles are the

Fabs, and the black dotted circles are the CDR. The red dots represent the N-glycosylations positions on the Fc. The orange star represents the exposed N-glycosylation position on PMB.

As any other proteins produced by eukaryotic cells, mAbs are subject to post-translational modifications (PTM), especially to N-glycosylations, which results from the formation of a covalent bond of an oligosaccharide with an asparagine residue[31] . This binding was shown to occur in a specific region corresponding to a consensus sequence, asparagine - X - serine/threonine[32] (X can be any amino acid except the proline). Several roles are attributed to the N-glycosylation considering the protein of interest[32–34]. Glycans chains can influence and regulate protein folding, thermal stability, protein function, expression, pH resistance, etc. About antibodies, most studies focus on N-glycosylations appearing in the Fc region[20,21,31], while the Fab region generally lacks glycosylation sites inherited from the germline (around 15–25% of IgG molecules found in serum possess one or more N-glycosylation sites within the variable regions of the Fab domain)[35]. Recent reviews have put forward the importance of glycosylation on antibody properties[36–41]. In particular, they have shown how this PTM on Fc enhances the ability of the mAb to bind to the different Fc receptors by reducing the flexibility of the Fc domain[17,38,42]. Interestingly, this reduction in flexibility has probably facilitated the determination of the majority of existing Fc structures as well as for the low number of mAbs full-length structures available[22,25,27,31]. In addition, because of their properties, glyco-engineering has become an important field for the design of antibodies, complementing the existing methods[26,43–46]. Sha et al. demonstrated that controlling fucosylation can enhance cytotoxicity[43] in the context of the destruction of a cancerous cell.

Several experimental studies exist, focusing on the effect of this PTM on the aggregation rate[39,42], its influence on the capacity to bind (either to their antigens or their Fc receptor) or its role in the Ab stability[39,45–47]. But, despite their importance and potential in antibodies engineering, only a limited numbers of studies have investigated the impact of the N-glycosylations on full-length IgG using *in silico* approaches. Among them, molecular dynamics simulations would be well adapted to bring a more comprehensive understanding of these effects across IgG subclasses and could help to explain phenomena observed experimentally [17,21,23,32,37].
Among the few computational studies, most of them have been restricted to isolated Fc fragments[37,42,47,48] and very few have considered a full-length antibody[38]. Only a full-length IgG1 model[20] was often studied, since it is the most present IgG[15,23], but other classes of IgG still exist in the PDB[21,22,31]. Some of these subclasses present significant structural differences in their architecture and carry different oligosaccharides compared to IgG1. These subclasses may therefore respond differently to the presence or absence of N-glycosylations.

Hence, the present article aims to study the effect of the N-glycosylations of two full-length mAbs of IgG2 and IgG4 classes, namely Mab231[21] and the Pembrolizumab[31] (PMB) respectively (Fig. 2), using *in silico* methodologies. A rapid comparison between them shows a relatively low sequence similarity (75%) for antibodies, where pairwise similarity typically reaches 90%[50]. They also adopt dissimilar 3D structures (Table S1). They both have their two N-glycosylations on their Fc domains but the glycosylation pattern is different between both mAb, as well in chemical composition as in its location (Fig. 1).

PMB is a monoclonal antibody, part of the IgG4 family, used against the Programmed-Death 1 (PD-1) in cancer treatment. It disables the ligand Programmed-Death Ligand 1 (PD-L1) to interact with PD-1, which allows the apoptosis of cancerous cells[31]. It presents two different oligosaccharides[31]. The anti-canine lymphoma Mab231, part of the IgG2 family, is used against canine lymphoma cancerous cells and non-Hodgkin's lymphoma cells[21]. Similarly to Pembrolizumab, it triggers the apoptosis of cancerous cells. It carries two identical oligosaccharide chains on its Fc region.

Both mAb were simulated with classical molecular dynamics simulation for a total time of 1.5 µs, with and without the full N-glycosylations chains as described in their initial structure deposited on the PDB. We performed an in-depth analysis to measure the impact of the N-glycosylations on the dynamics and the conformational space accessible to the protein by examining various properties, e.g preferred conformations, flexibility, local entropy of the residues to name a few.

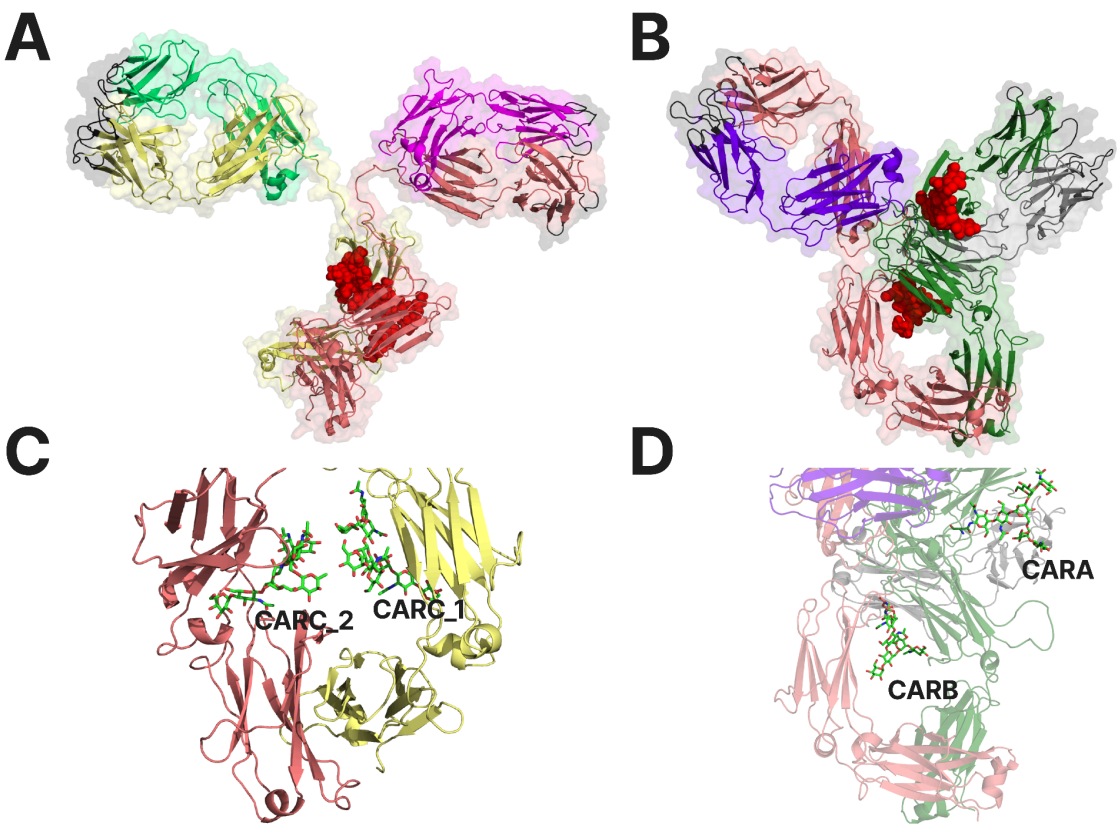

Figure 2: Top: 3D structures of Mab231 (PDB ID: 1IGT) A) and Pembrolizumab (PMB, PDB ID: 5DK3) B), left and right respectively. The chains are colored differently. For Mab231 (A), the pink and yellow chains are the heavy chains. The green and purple chains are the light chains. For PMB (B), the salmon and green chains are the heavy chains. The purple and grey chains are the light chains. The black zones correspond to the CDRs. In red, are indicated the sugars in space-filling representations. Bottom: Presentation of the structural difference of Pembrolizumab (C) and a "classic" structure of IgG represented by Mab231 (D). The green molecules represent the carbohydrates present in both crystallographic structures.

MATERIALS & METHODS.

Preparation of the initial structures.

The crystallographic full-length structures of the Pembrolizumab (PDB: 5DK3, 2.28 Å resolution, Scapin et al[31]), part of the IgG4 family and the Mab231 (PDB:1IGT, 2.8 Å resolution) were retrieved from the PDB web site (https://www.rcsb.org/).
The considered oligosaccharides for our study are presented as below:

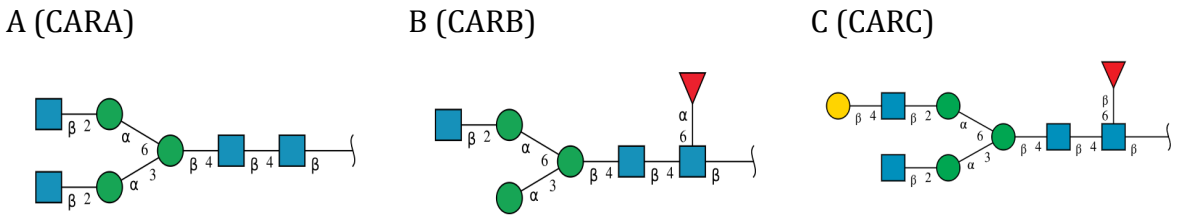

Figure 3: Schematic representation of the carbohydrates. A & B are from the Pembrolizumab (noted CARA and CARB in the following) Mab231 has twice the carbohydrate C (noted CARC_1 and CARC_2). Blue square stands for N-Acetyl Glucosamine (GlcNAc), green circle for mannose (Man), yellow circle for galactose (Gal), and red triangle for fucose (Fuc). Greek symbols indicate the anomeric form of the hemiacetal/hemiketal. The number at the connection line represents the position of alcoholic hydroxy where the glycosidic bond is formed. This schematic representation is based on *Symbol Nomenclature For Glycans*[50] (SNFG).

The domain delimitations of each antibody are defined in Table 1.

Table1: Delimitations of the fragments for pembrolizumab and Mab231 structure, with the location of the sugar. Subdomains of FAB-1 and FAB-2 are noted a and b respectively, in addition to the classical labelling.

		5DK3: PMB				1IGT: MAB231	
VLa	FAB-1	A	1-110	VLa	FAB-1	A	1-106
CLa(CL)			118-218 (109-214)	CLa(CL)			114-214
VHa		B	1-118	VHa		B	1-110
CH1a			127-220 (119-220)	CH1a			120-221
VLb	FAB-2	F	1-110	VLb	FAB-2	C	1-106
CLb2			118-218	CLb2			114-214
VHb		G	1-118	VHb		D	1-110
CH1b			127-220	CH1b			120-221
CH1_2 (CH2_a)	FC-1	B*	239-336 (234-341)	CH1_2 (CH2_a)	FC-1	B*	252-357
CH1_3 (CH3_a)			347-444 (342-446)	CH1_3 (CH3_a)			368-474
CH2_b	FC-2	G**	239-336	CH2_b	FC-2	D*	252-357
CH3_b			347-444	CH3_b			368-474
CARA	FC-1	B	N297	CARC_1	FC-1	B	N314
CARB	FC-2	G	N297	CARC_2	FC-2	D	N314

* Chain bound to sugars CARA and CARC_1 to their ASN on PMB and Mab231.
** Chain bound to sugar CARB and CARC_2 to their ASN on PMB and Mab231.

Completion of the structure.

The first step consisted of checking the integrity of the 3D structure. The 9 missing residues of PMB, located in the upper hinge region of both heavy chains (P230, A231, P232 on chain B; P230, A231, P232, E233, F234, L235 on chain G), were built with MODELLER using the automodel option. The initial parameters were used. 10 models were considered and the model with the best *DOPE*[51] scoring model used by MODELLER, was kept. This model was used for the systems with and without the N-glycosylation. Mab231 did not need any modelling since it was fully complete.

Alignment of sequences and structures of both antibodies: The sequence of the antibodies were compared, considering the light and heavy chain separately, using the Needleman-Wunsch implementation provided by the NIH website[52] with default parameters. The structural comparison was performed using the TM-align[53] tool. As for the sequence, the comparison was made chain by chain, light chains being compared one to another and similarly for the heavy chains.

System preparation and molecular dynamics protocol: The CHARMM-GUI[54] toolbox was used, especially the Solution Builder[54] tool to prepare the systems for molecular simulations. The following protocol has been realised for each system: i) the protonation states of each titratable amino acid were attributed using the internal tool from the CHARMM-GUI[55] toolbox for a pH of 7 from the "Solution Builder" tool, ii) the disulfide bonds indicated in the SSBND PDB fields were checked and added in each structure, iii) the systems including the glycosylated proteins were modelled using the internal tool 'Glycan Reader & Modeler' of the CHARMM-GUI suite, iv) each system was then placed within an explicit solvent cubic box filled with TIP3P water molecules and Na+ and Cl- ions corresponding to a salt concentration of 0.15 M plus the additional ions required to get a neutral system, v) the CHARMM-36 force field was chosen for the description of the atomistic interactions, vi) A minimization step using a steepest descent algorithm 5000 steps, with a force with force threshold convergence equals 100 kJ mol-1 nm-1. The bonds involving hydrogen atoms were constrained using the LINCS algorithm, which allowed an integration step of 2 fs, vii) the heating at 300K was performed in one step by attributing velocities randomly selected within a Maxwell-Boltzman distribution, the Parrinello-Rahman pressure control method was used at 1 bar, viii) the equilibration was performed over 125000 steps, each corresponding to a decreasing of force constraints on the heavy atoms. Each step was run for 10 nanoseconds and ix) the MD production was run without any restraint for 500 ns using GROMACS 2023.3. Three replicates corresponding to different initial velocities were performed. The glycosylated PMB system has a box of size (16.75 x 16.75 x 16.75 nm^3), the aglycosylated PMB has a box of size (17.34 x 17.34 x 17.34 nm^3). The glycosylated Mab231 (17.94 x 17.94 x 17.94 nm^3) and aglycosylated Mab231 is (17.95 x 17.95 x 17.95 nm^3). Long-range electrostatics were treated with particle-mesh Ewald method with a grid space of 0.12 nm. Temperature was controlled using a Nose-Hoover thermostat with a coupling constant of 0.1 ps.

Conformational and Dynamics Analysis: Most of the analyses were performed using GROMACS 2023.3 tools[56], e.g. *rms* tool for the Root Mean Square Deviation (RMSD) and *rmsf* tool, for the Root Mean Square Fluctuation (RMSF). RMSD was computed on the Cα using the whole mAbs, and only focusing on the Fab-1, Fab-2, Fc-1, and Fc-2 with each domain defined in *Table 1*. The RMSF was computed using the whole residues using the parameter *-res* of *rmsf* in GROMACS 2023.3. When required, the reference structure was chosen as the input conformation of the production step. Calculations were made for each trajectory. Average and standard deviations of the measures were also calculated over the three replicates.

Protein Blocks: We also considered another index of the flexibility, namely the N_{eq} of each amino acid[57]. This measure is defined as a conformational entropy that quantifies the conformational diversity adopted by an amino acid in a simulation. This measure is deduced from the analysis of the conformations adopted along the simulations in terms of a structural alphabet. This alphabet is composed of 16 letters (a to p), the protein

blocks (PBs)[58], each of these 16 PB letters were initially determined by regrouping similar local polypeptide backbone conformations of 5-residues length and defined by the φ,ψ dihedral angles. Each conformation extracted from the simulation is then translated into a suite of PB letters. The letter is attributed to the central residue. The four first and last residues of the considered protein are thus represented by the letter Z for completion purposes (with no physical meaning). For each amino acid, the frequency f_x of a given PB letter x is calculated over the whole set of frames of the trajectory. Then, the N_{eq} is calculated as a Shannon entropy index (Equation 1). Thus, the N_{eq} ranges between 1, i.e. the same state is observed all along the simulation and 16, i.e. the residue can adopt any state defined by the structural alphabet. This index informs on the deformability of a local region of the protein, where a value of 1 represents a rigid region and 16 a highly flexible region.

$$N_{eq} = exp(-\sum_{x=1}^{16} f_x lnf_x) \text{ Eq. 1}$$

Geometrical Analyses of the conformations: Antibodies are often described through common schematic shapes, e.g T-shape, Y-shape and a less popular one, λ-shape that are based essentially on the relative orientation of the Fab domains with respect to the Fc domain (Fig. S1). The orientation is defined by a set of angles, θ and φ, as proposed for example by Saporiti et al[20]. We defined θ_1, θ_2 as the angles between Fc and Fab1, Fab2 respectively (Fig. S1A). The origin of the coordinate system was the center of mass of the Hinge region, noted CoM-Hinge. We tested different definitions for the coordinate system axes. The z-axis was first defined as the vector joining the center of mass of the Hinge region to the CoM of the two CH2 domains. Alternatively, the principal inertia axis of the Fc domain was considered to define the z-axis. Similarly, the x-axis of the coordinate system was defined as the inertia axis of the Fab1 (Fab2) domain, or the vector joining CoM-Hinge to the center of mass of Fab1 (Fab2) (Fig. S1A). The y-axis was the axis perpendicular to the plane defined by z and x axes. The θ inter-Fab angle is computed as the angle between the two Fab inertia axes (Fig. S1A). We also examined the elbow angle that defines the potential crease between the variable and constant regions of the Fab domain (Fig. S1B). It is measured via center-of-mass vectors (VH→VL axis vs CH1→CL axis) as proposed by Stanfield *et al.* [58]. This value indicates the extent to which the Fab domain can be considered a rigid body. To complete the analysis, we finally measured the dihedral hinge angle of the two Fab arms around the Fc long axis. Detailed definitions are provided in the supplementary material (Fig. S1B & 1). To assess whether glycosylation significantly affects Fab conformational distributions, we performed statistical comparisons between glycosylated and non-glycosylated simulations. We checked the independence of the variables by calculating the autocorrelation time using block averages. Statistics were calculated over the effective number of samples. For angles treated as linear variables (θ F1/F2, θ Interfab, Elbow CM, Hinge Planar), we applied the Mann-Whitney U test[58]. For circular variables (φ F1/F2, Hinge Dihedral), we used the Watson-Wheeler test[59], which is appropriate for

periodic angular data. Additionally, Gaussian Mixture Models[60] were used in order to characterize groups of conformations on the angles basis.

Dynamic Cross Correlation Matrix (DCCM): The DCCM is a matrix which measures the correlation of the motion between each amino acid of the considered protein through the simulation. The Pearson Correlation method was used here to compute these correlations. First, the mean displacement vector for the amino acid is computed as follows.

$$\Delta r_i(t) = r_i(t) - \overline{r_i} \quad \text{Eq. 2}$$

where r_i is the vector of the position of the amino acid *i* at time *t*. And $\overline{ri}$ is the mean position for the amino acid *i*.
It is computed for each pair of amino acids. It is used to compute Pearson Correlation value as follows.

$$C_{ij} = \frac{\langle \mathbf{\Delta r}_i \cdot \mathbf{\Delta r}_j \rangle}{\sqrt{\langle \mathbf{\Delta r}_i^2 \rangle \langle \mathbf{\Delta r}_j^2 \rangle}} \quad \text{Eq. 3}$$

where Δri is the mean displacement vector of the amino acid *i*. Δrj is the mean displacement vector of the amino acid *j*. C_{ij} is the resulting value, the correlation between *i* and *j*.

The matrix was computed using the *Bio3D* library implemented in R.

Dimensional Reduction Tools:

- *Principal Component Analysis (PCA):* We first defined the set of residues that showed distinct correlation/anticorrelation values between the glycosylated and non-glycosylated states for PMB and Mab231 respectively based on the difference DCCM computed using the glycosylated and aglycosylated DCCM for each Mab231. We set the threshold for the absolute DCCM difference to 0.7 to select pairs of residues with markedly different correlation/anticorrelation between the two states. Since the number of residues impacted by the glycosylations are different between the mAbs, the number of pairs of residues is different between both mAbs. The ensemble of distances between the Cα atoms of these residues for each antibody was then calculated for all the recorded snapshots (50000) for the 3 replicates. These data were finally analysed with PCA, using the MDAnalysis, NumPy and Scikit-learn python packages.

- *T-SNE, UMAP and PacMAP:* We apply different transformations to the new data space computed with PCA, to more easily identify clusters of similar conformations depending on their glycosylation state. We first applied T-SNE[59] using the algorithm from scikit-learn, followed by UMAP algorithm[60]and PaCMAP[60] algorithm . All algorithms have been directly used on the PCA data.

Analysis of contacts between amino acids and carbohydrates. : The contacts between all amino acids but also between amino acids and the carbohydrates were calculated using the python library MDAnalysis for each calculation. A contact between two amino acids is defined if the distance between two Cα is equal or below 8 Å. The same criterion has been selected for the amino acids - carbohydrates contact, but with Cα and any heavy atom of the glycan chain. The count is normalized as follows.

$$\left(\frac{count\ of\ contacts}{trajectory\ time}\right) \times 100 \quad \text{Eq.4}$$

Allosteric network: The effect of glycans on allosteric networks was examined using the tool *allopath* developed by Delemotte et al[61,62]. (https://github.com/delemottelab/allosteric-pathways). The source was defined as the glycans, while the sink was the mAbs. For mutual information, the bootstrap set was fixed at 10, *n_blocks_col* and *n_blocks* parameters were set at 1 and *n_chains* at 1.

RESULTS

Since it was claimed in previous studies that the presence of sugars impacts the flexibility, we first examined whether this was the case for the two mAbs studied.

Do the sugars impact the flexibility and how?

Along the dynamics, the two proteins strongly deviate from their initial conformation with a global calculated RMSD for the full length antibody reaching 20-25 Å (Fig. S2). This corresponds to large conformational changes, slightly smaller for the glycosylated forms. However, the large values result from changes in the relative positioning of the Fc and Fab domains, which are not significantly deformed by themselves. (Fig. S2.) We can note more deformation for the Fc-1 for PMB.

The analysis of contacts along the simulations shows that some native contacts are lost but compensated by the formation of new contacts in both antibodies (Fig. S3). The presence of N-glycosylation tends to slightly limit the loss of native contacts for PMB (95% with sugar versus 88% without sugar). In the case of Mab231, the rate of native contacts remains very similar regardless of the presence or absence of sugar (~95%). Overall, contacts within subdomains are mainly maintained while new contacts are formed *between* the subdomains, induced by their relative motions.

These changes reflect the mechanical character of antibodies, namely rigid subdomains that move freely, thanks to the highly flexible hinges that connect them. This observation was also made for an IgG1 by Saporiti et al[20].

The two antibodies exhibit large average fluctuation profiles (Fig.4) but differ in the domains involved. For PMB, without glycan, the largest fluctuations are observed in the Fab domains compared to the Fc. The glycosylation reduces the fluctuations in the Fab while the Fc domain fluctuations are unchanged. In the case of Mab231 (Fig. 4B), the presence of glycans increases the fluctuation of the residues in the Fab-1 domain but decreases the fluctuations in the Fab-2 region. As for PMB, the fluctuations in the Fc domain remain the same on average.

When considering the overall flexibility as the cumulative RMSF, the glycosylation slightly reduces the total flexibility in both antibodies, although the effect remains modest.

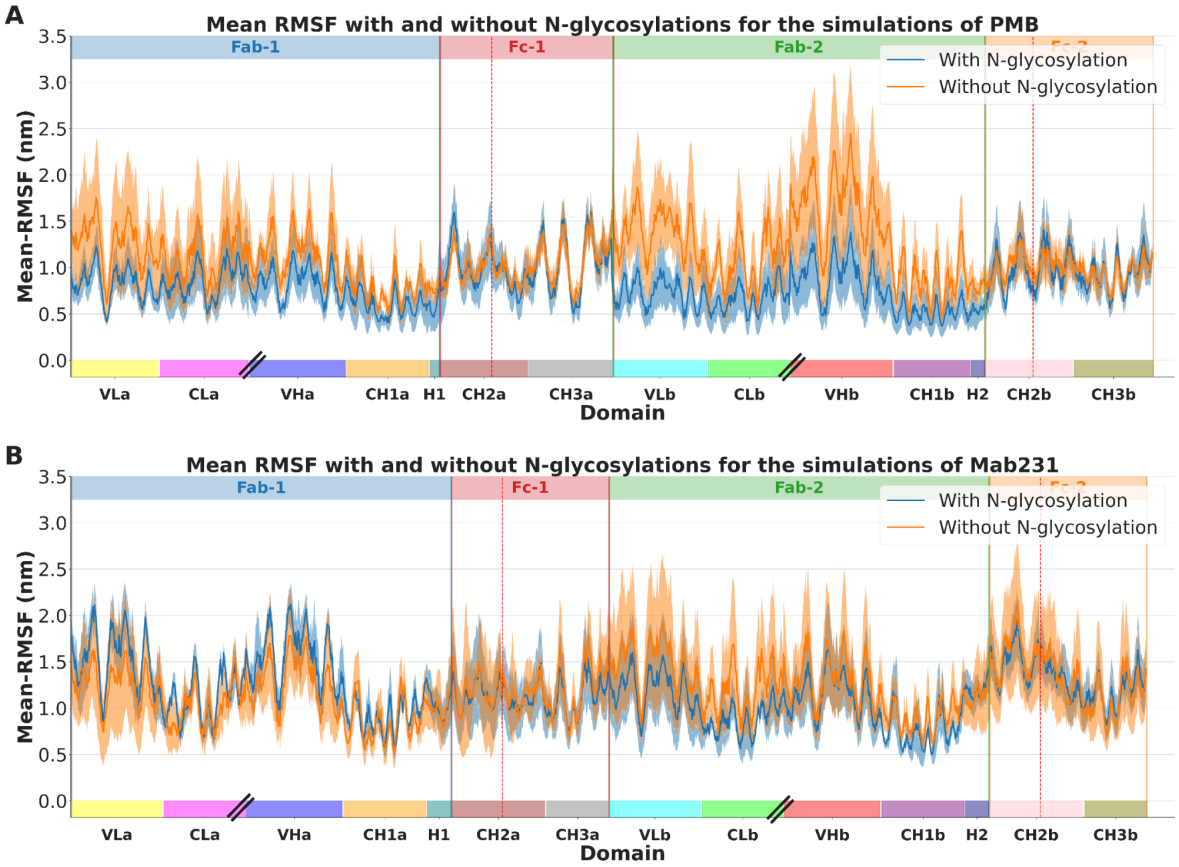

Figure 4: Mean RMSFs profiles for PMB (A) and Mab231 (B). The orange curve represents the mean RMSF without the N-glycosylation and the blue one, with the N-glycosylation. Each red line represents the position of the residue linked to the carbohydrate. Dash represents two domains that are disconnected in the structure.

Yet, to go further, we considered a measure, the N_{eq}, that may better reflect the diversity of local conformations in the two situations. This complements the RMSF that quantifies, on one hand, the amplitude of the variation of the position of a residue with respect to an average . On the other hand, the N_{eq} will be more appropriate to describe a

local level of flexibility. On average, the glycosylation slightly reduces the total N_{eq} for Mab231, whereas, interestingly, this value is slightly increased for glycosylated-PMB (Fig. S4). In the latter case, this increase is due to a few positions that can access a larger number of states (Fig S4) while other positions show a lower number of states.

To further investigate the dynamical cross-talk between subdomains, the dynamic cross-correlation matrix (DCCM) was calculated. It evaluates the correlated and anticorrelated motions between residues along the dynamics without and with the sugars.

The DCCMs calculated for each system show larger differences for Mab231 compared to PMB (Fig. S5). For both antibodies, the largest impact is observed between Fc-1 and Fab2 domains, where the presence of sugar induces new correlated motions (Fig. S5). For PMB (Fig. S5A & Fig. S5B), in presence of glycosylations, the correlated pairs of residues are mostly located around the hinge region and also on the heavy chains of the Fabs and Fc. In contrast, for Mab231, the removal of glycosylation results in correlated motions that are more localized, concentrating within specific subdomains such as the Fc and hinge regions rather than extending across the entire structure (Fig. S5C & Fig. S5D).

Examining the absolute differences of DCCMs between the glycosylated and aglycosylated antibodies allows to highlight the residues, and more precisely the subdomains that have markedly different behavior between the two states. For PMB for example, the CLb region relative to the CH2a region is the most affected by glycosylation states, along with the CH2a relative to CH1b (Fig. 5A). This is also true for Mab231 (Fig. 5B). For some subdomains, the differences are less marked but still present. For example, CLa with CH1a or CLb with VHb for PMB (Fig. 5A); CH1b and CLb or CH2b and CLb for Mab231 (Fig. 5B).

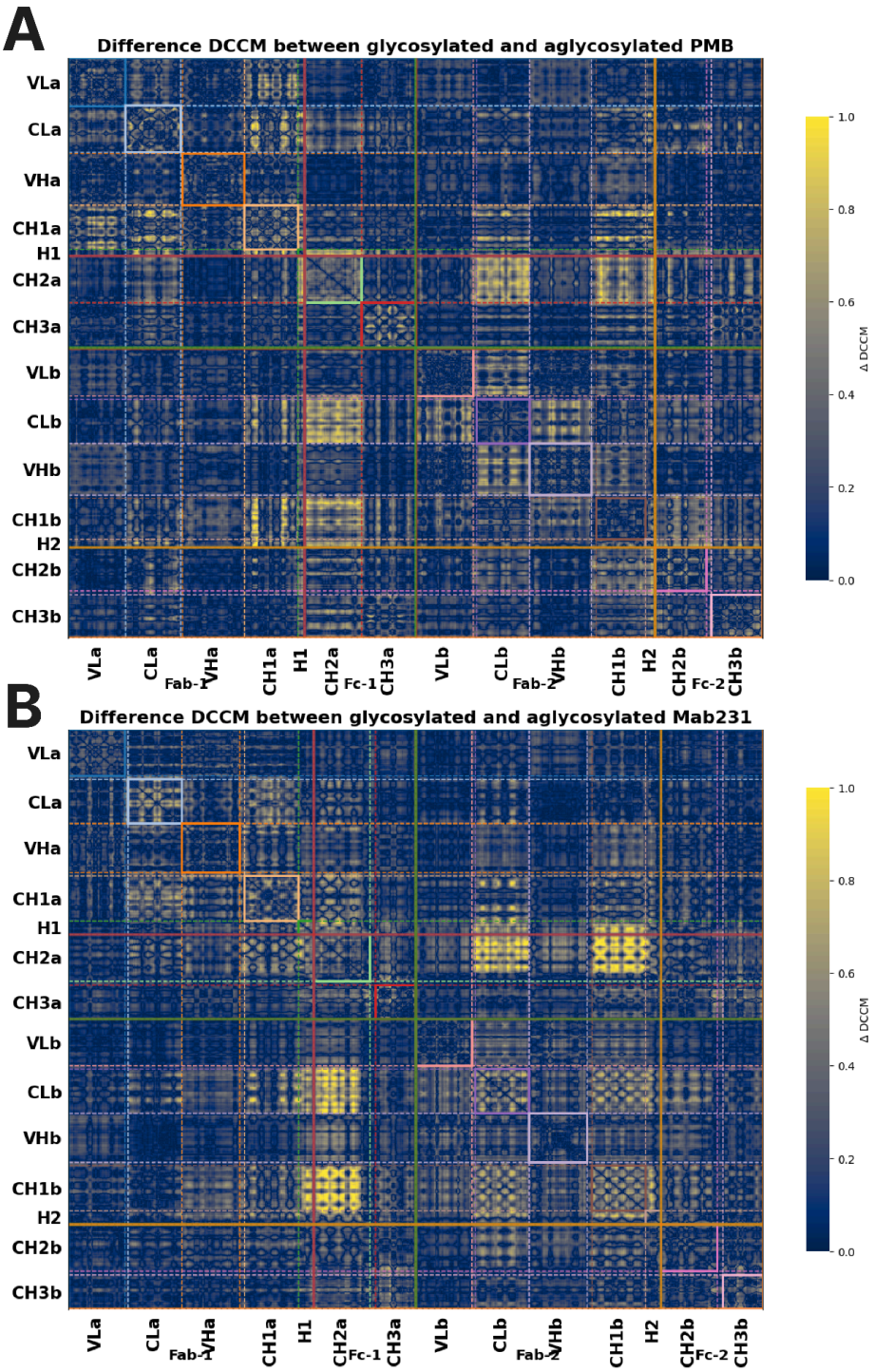

Figure 5: Difference DCCM computed using the DCCMs from the glycosylated and aglycosylated PMB (A) and Mab231 (B) simulations.

In summary, although the overall effect seems not huge, the presence of sugars still affects the flexibility of the proteins in some specific regions, especially in the connections between Fcs and Fabs.

Does the protein adopt preferred conformations depending on the glycosylated state?

Since the DCCM difference maps highlighted pairs of residues (Fig. 5 and Fig. S5) that appear influenced by the presence of glycans, we examined whether some conformations could be specific to the glycosylation state of the mAbs. Thus, we only selected the pairs of residues for which the difference is larger than 0.7 to further analyses. The distribution of distances between these pairs of residues was analysed using a principal component analysis. The projections of the conformations on the two first components (PC1 and PC2) are shown in Figure 6, colored according to the glycosylated state but also on their replicate origin.

For PMB (Fig. 6A), 9844 pairs of residues (~ 1/100 of the total pairs) were used and PC1 explains 74% of the variance. This figure shows that i) there is no clear separation between the glycosylated and non glycosylated state and ii) the conformations from different replicates for a given state are as distinct as between the two states, glycosylated and non glycosylated.
For Mab231, 15738 pairs of residues were used (Fig. 6B). Although the PC1 contribution to the total variance is smaller compared to PMB, (68%) and the conformations are more spread over the plane, the same conclusion can be drawn as for PMB: no clear distinction between the two glycosylation states emerges from the relative motions of the selected residue pairs. The same observation can be drawn whatever the threshold of 0.7 was used.

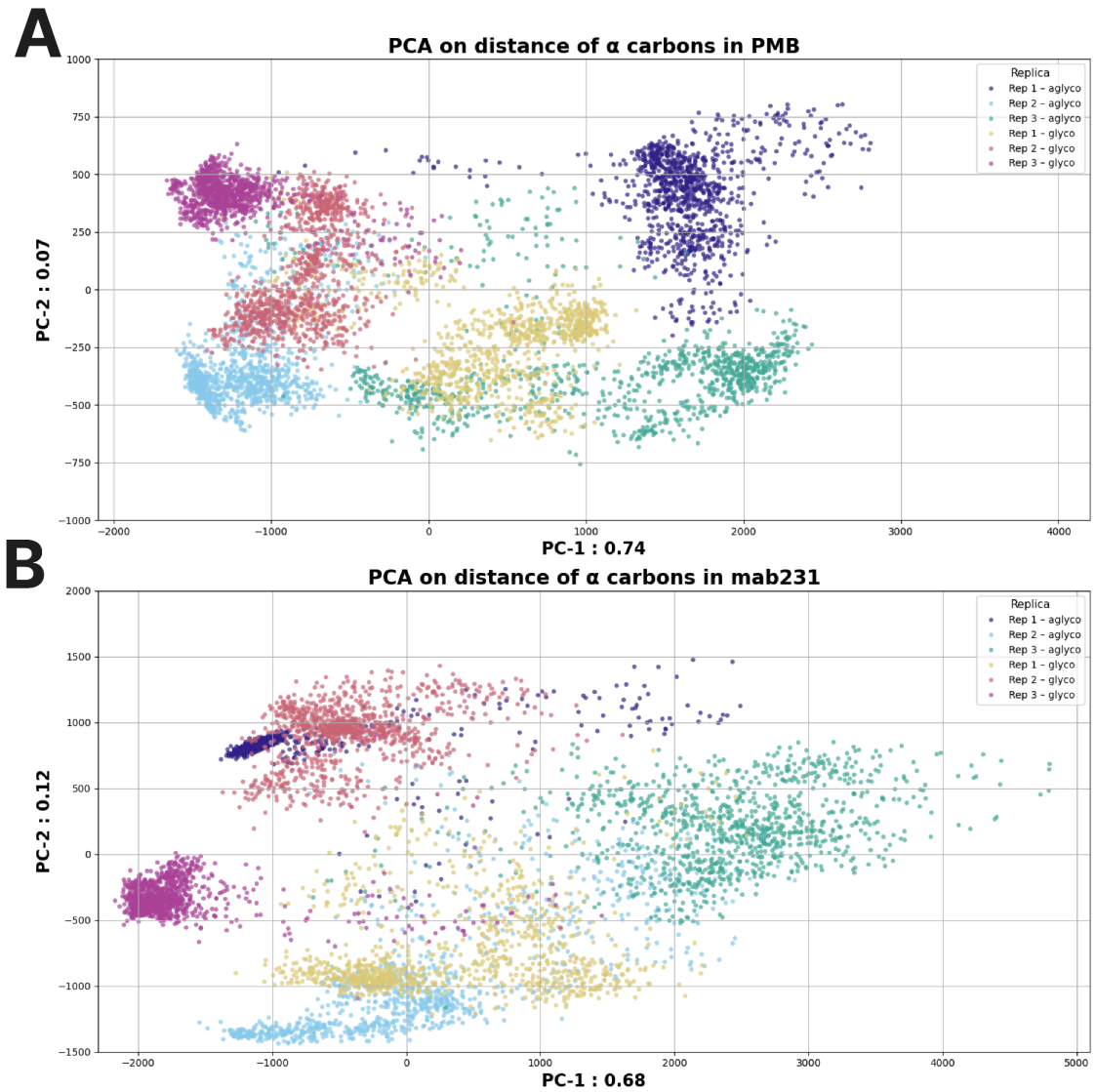

Figure 6: Projection of the two first principal components for PMB (A) and Mab231 (B). The data are colored according to the glycosylation state and the replicate origin.

We checked if these conclusions hold whatever the approach of dimension reduction used. We applied a PaCMAP analysis on the same set of Cα-Cα distances used in PCA. The approach is assumed to be appropriate for visualizing groups of data respecting short but also long distances among them, as in the original coordinate system[62,63]. The projection of the conformations on the two first components yielded by PaCMAP (Fig. S10) shows several groups for each state. Each group contains conformations from a given state, i.e. glycosylated and not glycosylated, which tends to indicate that the two forms visit different conformational landscapes. However, for a given state, the conformations extracted from the three replicates are spread over distinct groups. The distance between these groups is as large as between the clusters for each state. This is also confirmed by the t-SNE and UMAP analyses that identify overlapping groups containing conformations from both states (See Fig. S11 & Fig. S12). Therefore, based

on the distances considered, we cannot clearly distinguish the effect of the glycosylation, as already concluded by PCA analysis.
Overall, the glycosylation has no major effect on the conformation of the domains but slightly reduces the amplitude of the motions between domains.

In summary, we did observe global conformational changes when considering the RMSD and the evolution of native contacts for the two antibodies in both states. However, despite the extensive sampling, it was not possible to identify a clear effect of glycosylation on the *global* conformational landscape of either antibody. Nevertheless, we observed with the N_{eq}, the RMSF and the DCCM calculations that the addition of the glycans impacts *locally* the flexibility of the Ab and this effect depends on the Ab examined.

Finally, we examined alternative measures that might better characterize Ab conformations and the potential effect of glycans. Among the popular descriptors that were previously used to describe Ab conformations, we chose angles that describe the positioning of Fab domains with respect to the Fc domain. We considered θ_1, θ_2 defined as the angles between Fab1, Fab2 and Fc axes respectively, $\theta_{inter,}$ the angle between Fab1 and Fab2 axes, and φ_1, and φ_2 the rotation angles of Fab1, respectively Fab2, around the z axisangle.
The distribution of θ_1, θ_2 and θ inter and φ are given in Figure 7 for each Ab, with the measures of the statistical significance of the comparison. Statistical details are given in Table S2 & S3 for different geometrical features.For PMB, the distribution of angles θ_1, θ_2 and θ_{inter} varies depending on the glycosylation state for the two Fabs and the differences are statistically significant. For Mab231, the same observation can be drawn for θ_1, θ_2. For the θ_{inter} angle, differences exist between the two distributions and are statistically significant.

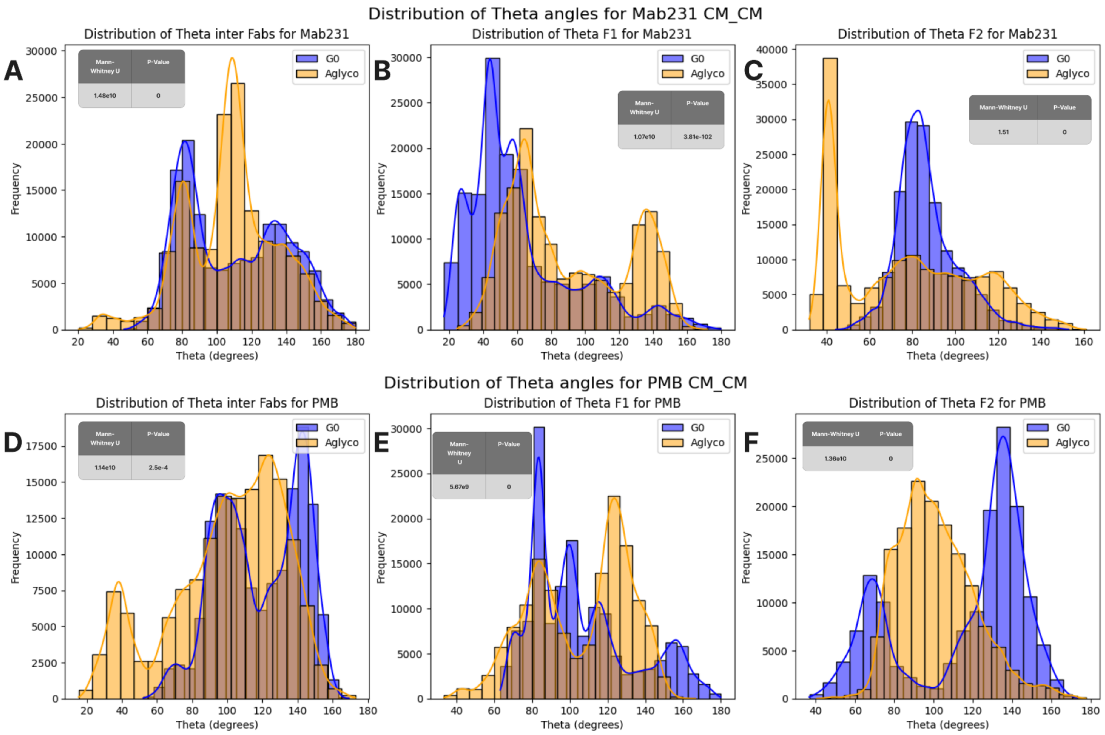

Figure 7: Distribution of theta Fab-1, Fab-2 and inter-Fab angles colored in red for aglycosylated and blue for glycosylated (G0) systems. For PMB Fab-1 (A), Fab-2 (B) and inter Fab (C) and Mab231 Fab-1 (D) Mab231 (E) and inter Fab Mab231 (F).

In summary, the glycosylation alters the conformational landscape of the Fabs with respect to the Fc domain. Note that these angles are frequently used to define canonical shapes of Ab, i.e T-shape, Y-shape and the less canonical one, λ-shape that we still observe rarely in simulation for Mab231 (Fig S8). Nevertheless, since such classifications rely on thresholds that vary across studies, we chose not to discuss changes in shape classification but provide illustrative results in the supplementary material.

Do and how do the sugars interact with the protein residues ?

The analyses presented above indicate that the carbohydrates do not significantly alter the overall dynamics of the protein but modulate the conformational regions explored, particularly the relative orientation of the Fab and Fc domains. These modifications could influence the protein's ability to interact with partners and *per se*, affect their functional properties. (Fig S9).

To further elucidate the potential impact of sugars on partner-interacting regions—the so-called "shielding effect"—we examined the specific residues in contact with different carbohydrates, as well as the persistence of these interactions. Figure 8 details the number of contacts between the carbohydrates and the various domains of the two Abs.

For easier visualization, the regions involved in these sugar-protein interactions are mapped onto the structures in Figure 9.

In the case of PMB, the highest number of contacts occurs between CARA and the CH2 residues of Fc–1, and between CARB and the CH2a residues of both the Fc-2 and Fc-1 domains; essentially, they interact primarily with the subdomains to which they are covalently bonded. Interestingly, a small number of contacts occur between CARA and certain Fab residues. This also occurs for CARB, though to a lesser extent. This is explained by PMB motions during the simulation, which brings Fc1 and Fab-1 into closer proximity, combined with a larger accessible conformational landscape for CARA due to its specific location (see Fig. 9). In contrast, CARB—sequestered between both Fc fragments (Fig. 2)—can rarely access the Fab regions. Beyond their spatial location, the chemical composition of the sugars (for instance, the presence of fucose and absence of mannose in CARB) may also contribute to these differences, as reported in previous studies[36,68,69] . Finally, a few contacts occur between the two sugars and the hinge regions, which could account for the slightly reduced flexibility observed in PMB in this region. (Fig. 4A).

For Mab231, a behavior similar to PMB is observed (Fig. 9B): each carbohydrate interacts mostly with its own domain and the facing Fc fragment. Both sugars exhibit a similar set of interactions due to their identical chemical composition. Notably, both sugars also interact with the Fab regions, though significantly less than in PMB. The conformational landscape of the two sugars is slightly reduced compared to CARA, which can be directly related to their symmetrical location in the core of the Fc fragments (Fig. 2).

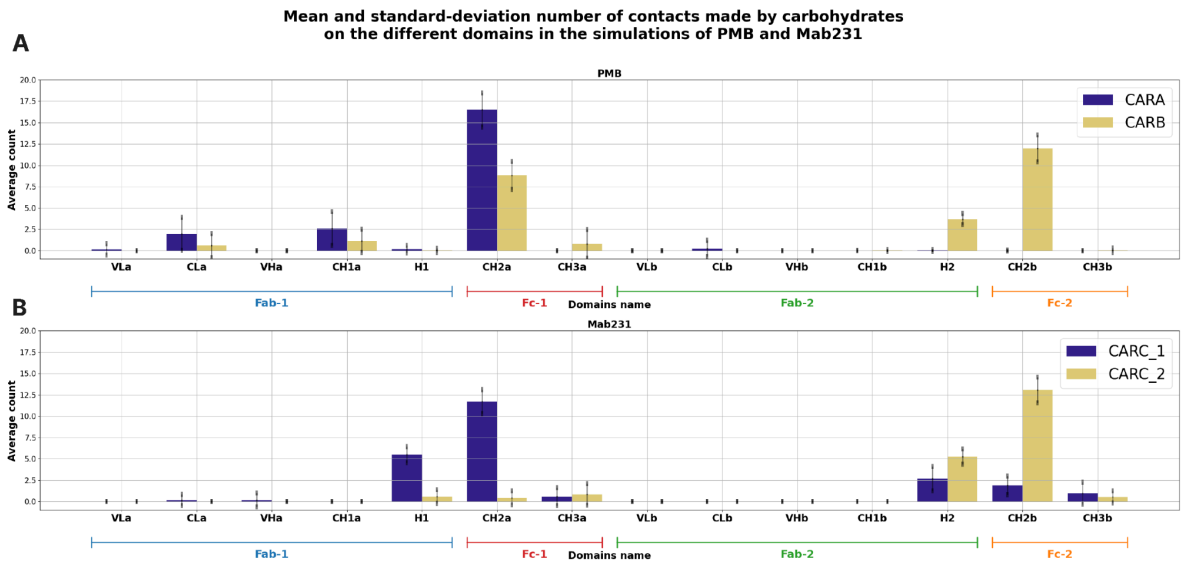

Figure 8: Average number of residues in interactions with the different carbohydrates in the simulations of PMB (A) and Mab231 (B). Both antibodies have two glycans, CARA from PMB in blue and CARB from PMB in orange. CARC_1 from Mab231 in blue and CARC_2 from Mab231 in orange.

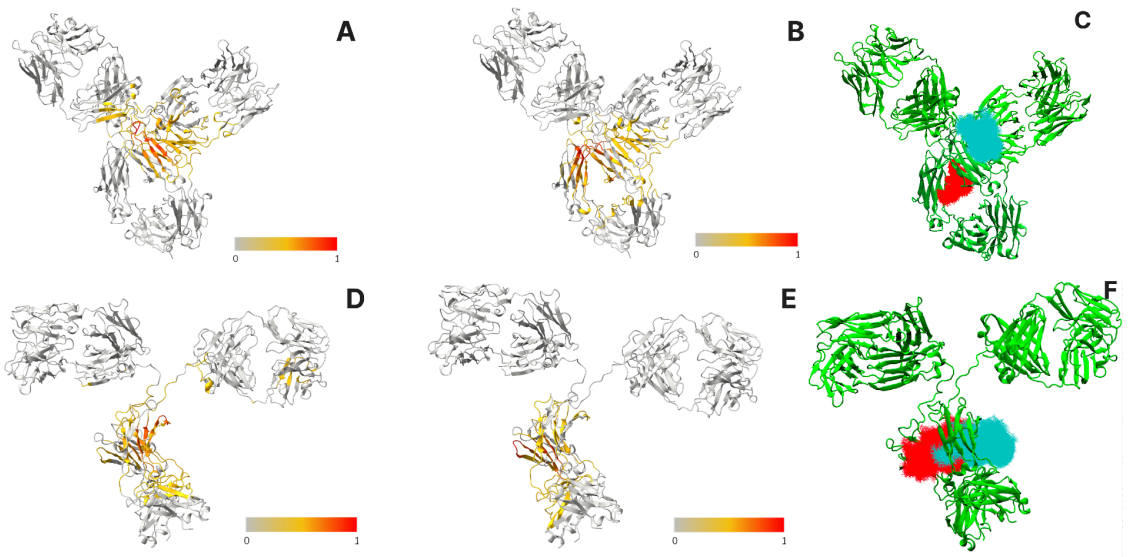

Figure 9: The interactions observed during all the simulations are projected on the crystallographic conformation for each mAb. Top) PMB residues in contact with A) CARA sugar and B) CARB sugar C) ensemble of conformations of the sugars CARA in cyan and CARB in red. Bottom) Mab231 residues in contact with D) CARC_1 sugar and E) CARC_2 sugar; F) ensemble of conformations of the sugars for CARC_1 and CARC_2, cyan and red respectively. The color bar represents the frequency of sugar contacts with the considered residue, from 0 (never in contact, in grey) to 1 (the most involved in contact with the glycan, in red).

The interactions detailed above are based on a distance criteria, which means *local* interaction since the threshold used is rather small. However, in the absence of any direct contact, the long-range impact of post-translational modifications has been previously demonstrated in several proteins, including Abs. Therefore, in order to evaluate this potential long-range effect, we examined the allosteric network using a dedicated tool[61,62], considering each glycan as a source. The residues involved in the allosteric network are displayed in Figure 10.

For PMB, the allosteric impact of CARA (Fig 10.A) extends well beyond the Fc domain, reaching the hinge region and the Fab domain, where several residues show high levels of involvement (indicated in orange). This is consistent with the contact analysis presented above, which identified direct interactions between CARA and Fab residues enabled by the conformational flexibility of this glycan. For CARB (Fig 10.B), the allosteric effect is predominantly concentrated on the Fc domain to which it is covalently attached, with a more limited contribution from the Fab domain compared to CARA. Again, this mirrors the contact analysis, where CARB, sequestered between the two Fc fragments, was found to rarely access the Fab regions.

For Mab231, both glycans (Fig 10.C & 10.D) have a similar effect that also extends to the variable regions of the Fab domains. Compared to PMB, all the contributions are generally less intense, but the structural coverage is much larger. Consequently, for both mAbs, the glycans appear to modulate the allosteric network not only within the Fc

domain but also in the Fab domains, which could influence antigen binding. Indeed, although the CDRs are not concerned by this allosteric effect, for Mab231, the structural core part of the Fab domain participates in this network. These residues, which are called “framework” residues, are known to play a role in the stabilization of the complex. In addition, the impact on the hinge region can be directly associated with the difference of mAbs general shape observed for both systems. This three-dimensional domain reorganization could also affect the binding properties of the mAbs towards their antigens and receptors.

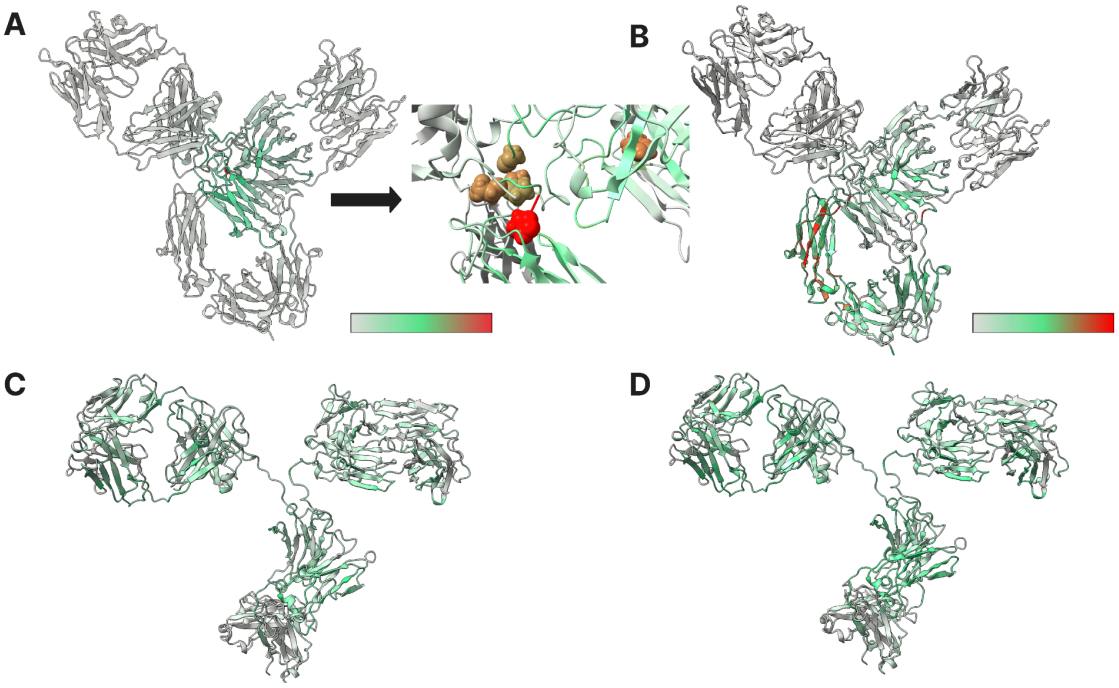

Figure 10: Projection of the implications of the residues in the allosteric network with the glycans as source. A) CARA on PMB. B) CARB on PMB. C) CARC_1 on Mab231. D) CARC_2 on Mab231. The color goes from grey to cyan to red. From the least information (0) at this residue to the most (max value depends on the system).

DISCUSSION

Until now, most of the theoretical and experimental studies mainly focus on the most abundant IgG class, namely IgG1. Moreover, in general, they restrict the exploration to the Fc domain that carries the glycosylation sites and interacts with the receptor. Consequently, the question of the Fc-glycosylation effect on the Fab domains is rarely addressed. To our knowledge, it is even less so for IgG2 and IgG4 that significantly differ from IgG1, in particular in the hinge region that connects Fab and Fc subdomains.
Therefore, the next sections will discuss the few studies done on the two antibodies examined in this paper in light of our own results and finally compared with the most abundant results obtained for IgG1 class.

The first molecular dynamics simulations on the Mab231 IgG2 were performed by Wang et al.[63], who investigated different systems ranging from the full-length glycosylated form of the protein to single subdomains. The simulation time length was limited to 40 ns. They noted similar backbone fluctuations for the glycosylated and aglycosylated full-length systems except in the CH2 domains. They also remarked that in the absence of the other domains of the mAbs, i.e CH3, Fabs and hinge domains, the absence of glycosylation has a significant impact on the structural stability of the CH2 domains, similar to a temperature stress. Although the secondary structures were maintained, the tertiary and quaternary structures of these domains were affected, the two CH2 moves in respect to each other when glycans are missing, leading to a solvent exposure of a region, defined as prone to aggregation in the article. This could suggest the sampling of a more "open form" of the Mab231, that is supposed to be required for Fc-receptor binding.

More recently, Ma[66] examined the dynamics of glycans in Mab231 and the putative impact of the antigen and receptor binding on their dynamics. The results, which mainly focused on changes of distances between the glycans themselves, and carbohydrates with CH3 domains, showed that the presence of partners changes slightly these distances. Since we did not explore explicitly the impact of partner binding, we could not compare with these results directly. However, as we observed an equilibrium between two distinct and well separated distance distributions (Fig S13), the "simple" dynamics of the glycosylated system would be sufficient for the Ab to adapt to receptor binding, if the above cited "open form" would be required as discussed in several publications. Despite its interest, this discussion relies on the definition of the distance itself to characterize those different conformations of the Fcs, which is actually questionable. In the case of IgG1, the residue P238 is often used for defining the aperture but in the case of IgG2, this residue is absent. Moreover, this residue is located in the flexible hinge region.

In the case of the IgG4 pembrolizumab, Natesan and Agrawal[67] compared the dynamics of PMB with an IgG1 using molecular dynamics simulations in implicit solvent. They considered the same glycosylation for the two systems, i.e. a A2G0 glycan which is the most simplified model of glycans[67]. Unfortunately, they did not address the question of the glycosylation itself but mainly examined the impact of the starting conformation on the dynamics. Thus, we can essentially notice that the conformations adopted by IgG4 are very diverse, in particular the relative positioning of Fabs versus Fc, as we observed in our own simulations.

Spiteri et al.[68] provided useful insights on the role of Fc glycosylation in IgG4 using a combination of experimental approaches, and Monte Carlo (MC) simulations. When considering solution X-ray diffusion or neutron scattering results, they observed minor differences in the radius of gyration or the relative distance between Fabs subunits, Fc subunits and Fab-Fc subunits. This means that, at a macroscopic level, no major differences can be observed between the two states. However, the neutron experimental data indicated more degrees of freedom for the aglycosylated form compared to the glycosylated one.Using MC simulations, they built atomistic models and generated a

large set of conformations that fit experimental data and confirmed that in the aglycosylated systems, the Fc domain can adopt a larger conformational diversity compared to the glycosylated system. This result agrees with our own results obtained from the angular analysis (Fig 7) that shows different Fab orientation relative to the Fc domain depending on the glycosylation state. The increasing of the number of degrees of freedom can also be related to the increasing of the local flexibility captured by the N_{eq} and RMSF metrics for the aglycosylated system (Figs. 4 & S4).
Without addressing the question of glycosylation, Tarenzi et al[69] have nevertheless investigated the aglycosylated form of Pembrolizumab in absence (apo state) and presence of the target protein PD-1 (holo state) using all-atom molecular dynamics simulations. Thus, their results for the apo state can be compared to our own results on aglycosylated PMB. Based on the RMSD between structures, they grouped the all frames in 5 clusters that display a different set of contacts between Fab1, Fab2 and Fc. Whatever the cluster, they identified networks of interactions that join residues in the Fc domain to residues in Fab1 or Fab2, along a pathway that transits through the hinge.
This information network is similar to our own results, which can thus be considered as a hallmark of the PMB.

Comparison with a IgG1 study
As aforementioned, most of the studies have been conducted on IgG1 but a few of them have considered the full length of the Ab. Zhang et al[42] investigated the impact of glycosylation on the conformational dynamics of an IgG1 Fc domain. They demonstrated that the absence of glycans on the CH2 domains allows the chains to move closer during the simulations,whereas glycosylation maintains a greater inter-CH2 distance. In our study, no major impact on the intrinsic flexibility of CH2 domains was observed for Mab231 but we did also notice changes in the distances between the two CH2, depending on the presence or absence of the sugars (Fig. S13B). Specifically, the glycosylated form of Mab231 is characterised by two states as populated, with slightly smaller distances than in the X-ray structure. The first group (distance ~37 Å) would correspond to a more opened form whereas the second group (distance ~ 33 Å) would be a closer one. In the aglycosylated system, we observe only one group, with distances intermediate compared to the glycosylated system. The large sampling we performed, with longer MD, enabled us to observe closer and more open forms in the glycosylated system, which could be indicative of a “breathing motion” of the Fc domain in Mab231.

Similarly, Subedi and Barb[70] used NMR spectroscopy on an isolated IgG1 Fc fragment to explore the effect of the N-glycosylation. They showed that it helps the interaction between the Fc and its receptor. Indeed, it does not alter Fc quaternary structure but stabilizes the C'E loop that bears the glycosylation (residues 280 to 297 in IgG1, equivalent to the same region in PMB) and belongs to the binding interface with the receptor FcγRIIIa. Overall, they observed a strong correlation between the loop conformation and the receptor affinity.

Our results on full-length PMB and Mab231 confirm the absence of a major effect of the glycosylation on the quaternary structure but do not show major changes in the flexibility in this C'E loop. Beside the difference in the Fc sequences, the presence of Fabs and hinge domains might explain the differences observed between the two studies. Among the very few studies that explore the impact of glycosylation on full-length Ab, the work performed by Saporiti et al[20] has brought important insights on the role of sugar on adalimumab, a IgG1 class antibody. They built the whole system as a homology model based on the combination of two X-ray structures. They considered three different systems: a glycosylated afucosylated form, glycosylated fucosylated form and the aglycosylated form. Similar to our work here, they ran long molecular dynamics simulations of 1µs with 3 replicas for each adalimumab model in explicit water. They observed that the flexibility of the CH2 is rather similar whether the presence or not of a sugar, except in the very first part of the region which is disordered since it is linked to the hinge domain and thus, much more flexible, for the glycosylated afucosylated form. They also examined the question of the opening or closure of the Fc domain. They found that the absence of sugar or the presence of fucose on the sugar leads to a more compact Fc domain, suggesting a closed structure. Note that they used the distance between the two ASN bearing the sugars to probe this feature. Interestingly, the addition of the fucose to the carbohydrate chain seems to allow the CH2 domains to get closer. These deformations act directly on the ability of the adalimumab to interact with its receptor, especially around the CH2 region. The afucosylated glycan would maintain an open conformation of the Fc. Thus, residues are more exposed to the solvent and might be available for the interaction as seen in the works realized by Wang et al[71]. For PMB, we observe a similar tendency when the same criteria is considered, but the fucose is only present on the CARB (Fig. S13A). For Mab231, which also includes a fucose in both glycans, we observed that the distributions are rather similar between the two systems (Fig. S13B). Therefore, we cannot draw a conclusion regarding such a closing effect. In contrast, when the center of mass of the CH2 domain is used as a measure (Fig. S13C & S13D), the distribution changes and the conclusions are as follows: i) the presence of the glycosylation decreases the CoM distance compared to the X-ray structure, ii) two main states can be observed in the glycosylated form, one being more open than the other and iii) the aglycosylated form is in between. Therefore, we can't draw a definite conclusion on the effect of glycosylation on the opening of the Fc domain for Mab231 since it depends on the reference chosen. This reflects the difficulty of fully characterizing the open and closed states, since the structural references differ substantially between IgG subclasses.

In summary, our results show that the glycans can affect the relative conformations visited by Fc or Fab domain, on the basis of angle distribution analysis, but not necessarily in the same way as observed for some IgG1[38,67]. However, we noted that the glycans could have an impact on the allosteric network of the antibodies ,which could potentially modify the capacity to interact with the receptor or the antigen, and consequently affect their biological functions. Interestingly, Subedi and Barb (2015)[71],

who used experimental approaches to decipher the mechanism behind the allosteric modulation caused by the N-glycosylations on the IgG1 Fc domain, precisely observed structural perturbation on loop regions. Unfortunately, since they only worked on the Fc domain of an IgG1, they could not observe the potential allosteric mechanism on the Fab domains as we noted for PMB and Mab231, which could be an explanation of the results presented in this article.

CONCLUSION

In this work, we report a comprehensive study that explores and compares the effect of the N-glycosylations on the behavior of two full-length mAbs, the Pembrolizumab, an IgG4, and the Mab231 an IgG2, using all-atoms molecular dynamics simulations.

This study allowed us to highlight the similarities and differences relative to their different glycosylation patterns, but also to their sequence and conformational characteristics, in particular the cross-talk between the subdomains composing the protein. First of all, despite having an initial different shape related to the length difference of the hinge region, we confirmed that both Abs are very flexible objects that exhibit large conformational changes all along the dynamics. In both cases, regardless of the presence of sugars, native contacts are lost but compensated by the formation of new contacts that maintain the overall structural stability. In contrast, we showed that the glycosylation does impact the flexibility of PMB and Mab231 differently, but moderately. For PMB, only the Fabs domains are affected by the presence of glycosylation by locally reducing their flexibility, while the dynamical profile remains similar for the Fc region. Mab231 appears less affected by glycosylation, irrespective of whether the Fab or Fc domains are considered.

However, the large inherent flexibility of the sugars allows them to interact with several residues, even far from the glycosylation site, which in turn modifies the correlated motions between residues in both PMB and Mab231. Considering the size of the systems and their highly dynamical properties, care should be taken to clearly settle the impact of the glycosylation. Nevertheless, considering different geometrical characteristics and performing careful analyses of our MD data, we have shown that some parts of the two mAbs are *significantly* impacted by the presence of the sugars. This is the case for the relative orientation of the Fab regions with respect to the Fc domains. Importantly, we highlighted that the effect of the glycans on the allosteric network of both antibodies were not limited to the Fc domains but also to the Fabs. The effects were different for both mAbs. This might be due to the nature of the sugar, and/or to the linker region that will influence the overall conformations. To settle their respective role, it would be necessary to examine alternative glycosylations. In any case, the long range effect that we highlight might have an influence on the paratope region and consequently to the capacity or the way to bind the antigen. Future studies should therefore extend this analysis to additional IgG isotypes and alternative glycan compositions. Finally, our study shows that the presence of the sugars on a full-length antibody IgG4 and IgG2 does not necessarily provoke an opening of the two CH2 of Fc domain, which is supposed to be important for the binding with the receptor. Therefore, including the

Fc-receptor in the simulations would be of interest to clarify the role of the glycans on the binding of the antibody with its receptor.

Bibliography.

(1) Li, W.; Prabakaran, P.; Chen, W.; Zhu, Z.; Feng, Y.; Dimitrov, D. Antibody Aggregation: Insights from Sequence and Structure. *Antibodies* **2016**, *5* (3), 19. https://doi.org/10.3390/antib5030019.

(2) Dillman, R. O. Monoclonal Antibodies for Treating Cancer. *Ann. Intern. Med.* **1989**, *111* (7), 592–603. https://doi.org/10.7326/0003-4819-111-7-592.

(3) Berger, M.; Shankar, V.; Vafai, A. Therapeutic Applications of Monoclonal Antibodies. *Am. J. Med. Sci.* **2002**, *324* (1), 14–30. https://doi.org/10.1097/00000441-200207000-00004.

(4) Waldmann, T. A. Monoclonal Antibodies in Diagnosis and Therapy. *Science* **1991**, *252* (5013), 1657–1662. https://doi.org/10.1126/science.2047874.

(5) Kennedy, P. J.; Oliveira, C.; Granja, P. L.; Sarmento, B. Monoclonal Antibodies: Technologies for Early Discovery and Engineering. *Crit. Rev. Biotechnol.* **2018**, *38* (3), 394–408. https://doi.org/10.1080/07388551.2017.1357002.

(6) Vaickus, L.; Foon, K. A. Biotechnology Update: Overview of Monoclonal Antibodies in the Diagnosis and Therapy of Cancer. *Cancer Invest.* **1991**, *9* (2), 195–209. https://doi.org/10.3109/07357909109044230.

(7) Reichert, J. M.; Valge-Archer, V. E. Development Trends for Monoclonal Antibody Cancer Therapeutics. *Nat. Rev. Drug Discov.* **2007**, *6* (5), 349–356. https://doi.org/10.1038/nrd2241.

(8) Adams, G. P.; Weiner, L. M. Monoclonal Antibody Therapy of Cancer. *Nat. Biotechnol.* **2005**, *23* (9), 1147–1157. https://doi.org/10.1038/nbt1137.

(9) Jabbour, E.; O'Brien, S.; Ravandi, F.; Kantarjian, H. Monoclonal Antibodies in Acute Lymphoblastic Leukemia. *Blood* **2015**, *125* (26), 4010–4016. https://doi.org/10.1182/blood-2014-08-596403.

(10) Majeti, R. Monoclonal Antibody Therapy Directed against Human Acute Myeloid Leukemia Stem Cells. *Oncogene* **2011**, *30* (9), 1009–1019. https://doi.org/10.1038/onc.2010.511.

(11) Grossbard, M.; Press, O.; Appelbaum, F.; Bernstein, I.; Nadler, L. Monoclonal Antibody-Based Therapies of Leukemia and Lymphoma. *Blood* **1992**, *80* (4), 863–878. https://doi.org/10.1182/blood.V80.4.863.863.

(12) Ritz, J.; Schlossman, S. Utilization of Monoclonal Antibodies in the Treatment of Leukemia and Lymphoma. *Blood* **1982**, *59* (1), 1–11. https://doi.org/10.1182/blood.V59.1.1.1.

(13) Portetelle, D.; Bruck, C.; Mammerickx, M.; Burny, A. Use of Monoclonal Antibody in an ELISA Test for the Detection of Antibodies to Bovine Leukaemia Virus. *J. Virol. Methods* **1983**, *6* (1), 19–29. https://doi.org/10.1016/0166-0934(83)90064-2.

(14) Albitar, M. *Monoclonal Antibodies: Methods and Protocols*; Springer Science & Business Media, 2007.

(15) Yokoyama, W. M.; Christensen, M.; Santos, G. D.; Miller, D.; Ho, J.; Wu, T.; Dziegelewski, M.; Neethling, F. A. Production of Monoclonal Antibodies. *Curr. Protoc. Immunol.* **2013**, *102*, 2.5.1-2.5.29. https://doi.org/10.1002/0471142735.im0205s102.

(16) Rita Costa, A.; Elisa Rodrigues, M.; Henriques, M.; Azeredo, J.; Oliveira, R. Guidelines to Cell Engineering for Monoclonal Antibody Production. *Eur. J.*

Pharm. Biopharm. Off. J. Arbeitsgemeinschaft Pharm. Verfahrenstechnik EV **2010**, *74* (2), 127–138. https://doi.org/10.1016/j.ejpb.2009.10.002.
(17) Liu, L. Antibody Glycosylation and Its Impact on the Pharmacokinetics and Pharmacodynamics of Monoclonal Antibodies and Fc-Fusion Proteins. *J. Pharm. Sci.* **2015**, *104* (6), 1866–1884. https://doi.org/10.1002/jps.24444.
(18) García Merino, A. Monoclonal Antibodies. Basic Features. *Neurol. Engl. Ed.* **2011**, *26* (5), 301–306. https://doi.org/10.1016/S2173-5808(11)70063-3.
(19) Maynard, J.; Georgiou, G. Antibody Engineering. *Annu. Rev. Biomed. Eng.* **2000**, *2*, 339–376. https://doi.org/10.1146/annurev.bioeng.2.1.339.
(20) Saporiti, S.; Parravicini, C.; Pergola, C.; Guerrini, U.; Rossi, M.; Centola, F.; Eberini, I. IgG1 Conformational Behavior: Elucidation of the N-Glycosylation Role via Molecular Dynamics. *Biophys. J.* **2021**, *120* (23), 5355–5370. https://doi.org/10.1016/j.bpj.2021.10.026.
(21) Harris, L. J.; Larson, S. B.; Hasel, K. W.; McPherson, A. Refined Structure of an Intact IgG2a Monoclonal Antibody. *Biochemistry* **1997**, *36* (7), 1581–1597. https://doi.org/10.1021/bi962514+.
(22) Blech, M.; Hörer, S.; Kuhn, A. B.; Kube, S.; Göddeke, H.; Kiefer, H.; Zang, Y.; Alber, Y.; Kast, S. M.; Westermann, M.; Tully, M. D.; Schäfer, L. V.; Garidel, P. Structure of a Therapeutic Full-Length Anti-NPRA IgG4 Antibody: Dissecting Conformational Diversity. *Biophys. J.* **2019**, *116* (9), 1637–1649. https://doi.org/10.1016/j.bpj.2019.03.036.
(23) Chames, P.; Van Regenmortel, M.; Weiss, E.; Baty, D. Therapeutic Antibodies: Successes, Limitations and Hopes for the Future. *Br. J. Pharmacol.* **2009**, *157* (2), 220–233. https://doi.org/10.1111/j.1476-5381.2009.00190.x.
(24) Pang, K. T.; Yang, Y. S.; Zhang, W.; Ho, Y. S.; Sormanni, P.; Michaels, T. C. T.; Walsh, I.; Chia, S. Understanding and Controlling the Molecular Mechanisms of Protein Aggregation in mAb Therapeutics. *Biotechnol. Adv.* **2023**, *67*, 108192. https://doi.org/10.1016/j.biotechadv.2023.108192.
(25) Gallagher, D. T.; Galvin, C. V.; Karageorgos, I. Structure of the Fc Fragment of the NIST Reference Antibody RM8671. *Acta Crystallogr. Sect. F Struct. Biol. Commun.* **2018**, *74* (9), 524–529. https://doi.org/10.1107/S2053230X18009834.
(26) García-Alija, M.; Van Moer, B.; Sastre, D. E.; Azzam, T.; Du, J. J.; Trastoy, B.; Callewaert, N.; Sundberg, E. J.; Guerin, M. E. Modulating Antibody Effector Functions by Fc Glycoengineering. *Biotechnol. Adv.* **2023**, *67*, 108201. https://doi.org/10.1016/j.biotechadv.2023.108201.
(27) Deisenhofer, J. Crystallographic Refinement and Atomic Models of a Human Fc Fragment and Its Complex with Fragment B of Protein A from Staphylococcus Aureus at 2.9- and 2.8-.ANG. Resolution. *Biochemistry* **1981**, *20* (9), 2361–2370. https://doi.org/10.1021/bi00512a001.
(28) Yanaka, S.; Yogo, R.; Kato, K. Biophysical Characterization of Dynamic Structures of Immunoglobulin G. *Biophys. Rev.* **2020**, *12* (3), 637–645. https://doi.org/10.1007/s12551-020-00698-1.
(29) Berman, H. M.; Westbrook, J.; Feng, Z.; Gilliland, G.; Bhat, T. N.; Weissig, H.; Shindyalov, I. N.; Bourne, P. E. The Protein Data Bank. *Nucleic Acids Res.* **2000**, *28* (1), 235–242. https://doi.org/10.1093/nar/28.1.235.
(30) Griffin, L.; Lawson, A. Antibody Fragments as Tools in Crystallography. *Clin. Exp. Immunol.* **2011**, *165* (3), 285–291. https://doi.org/10.1111/j.1365-2249.2011.04427.x.
(31) Scapin, G.; Yang, X.; Prosise, W. W.; McCoy, M.; Reichert, P.; Johnston, J. M.; Kashi, R. S.; Strickland, C. Structure of Full-Length Human Anti-PD1

Therapeutic IgG4 Antibody Pembrolizumab. *Nat. Struct. Mol. Biol.* **2015**, *22* (12), 953–958. https://doi.org/10.1038/nsmb.3129.
(32) Hirata, T.; Kizuka, Y. N-Glycosylation. In *The Role of Glycosylation in Health and Disease*; Lauc, G., Trbojević-Akmačić, I., Eds.; Advances in Experimental Medicine and Biology; Springer International Publishing: Cham, 2021; Vol. 1325, pp 3–24. https://doi.org/10.1007/978-3-030-70115-4_1.
(33) Montefiori, D. C.; Robinson, W. E.; Mitchell, W. M. Role of Protein N-Glycosylation in Pathogenesis of Human Immunodeficiency Virus Type 1. *Proc. Natl. Acad. Sci.* **1988**, *85* (23), 9248–9252. https://doi.org/10.1073/pnas.85.23.9248.
(34) Gu, J.; Isaji, T.; Xu, Q.; Kariya, Y.; Gu, W.; Fukuda, T.; Du, Y. Potential Roles of N-Glycosylation in Cell Adhesion. *Glycoconj. J.* **2012**, *29* (8–9), 599–607. https://doi.org/10.1007/s10719-012-9386-1.
(35) van de Bovenkamp, F. S.; Hafkenscheid, L.; Rispens, T.; Rombouts, Y. The Emerging Importance of IgG Fab Glycosylation in Immunity. *J. Immunol.* **2016**, *196* (4), 1435–1441. https://doi.org/10.4049/jimmunol.1502136.
(36) Wolf, B.; Piksa, M.; Beley, I.; Patoux, A.; Besson, T.; Cordier, V.; Voedisch, B.; Schindler, P.; Stöllner, D.; Perrot, L.; Von Gunten, S.; Brees, D.; Kammüller, M. Therapeutic Antibody Glycosylation Impacts Antigen Recognition and Immunogenicity. *Immunology* **2022**, *166* (3), 380–407. https://doi.org/10.1111/imm.13481.
(37) Xiong, Y.; Karuppanan, K.; Bernardi, A.; Li, Q.; Kommineni, V.; Dandekar, A. M.; Lebrilla, C. B.; Faller, R.; McDonald, K. A.; Nandi, S. Effects of N-Glycosylation on the Structure, Function, and Stability of a Plant-Made Fc-Fusion Anthrax Decoy Protein. *Front. Plant Sci.* **2019**, *10*, 768. https://doi.org/10.3389/fpls.2019.00768.
(38) Wada, R.; Matsui, M.; Kawasaki, N. Influence of N-Glycosylation on Effector Functions and Thermal Stability of Glycoengineered IgG1 Monoclonal Antibody with Homogeneous Glycoforms. *mAbs* **2018**, *11* (2), 350–372. https://doi.org/10.1080/19420862.2018.1551044.
(39) Ivarsson, M.; Villiger, T. K.; Morbidelli, M.; Soos, M. Evaluating the Impact of Cell Culture Process Parameters on Monoclonal Antibody N-Glycosylation. *J. Biotechnol.* **2014**, *188*, 88–96. https://doi.org/10.1016/j.jbiotec.2014.08.026.
(40) Plavša, B.; Rudman, N.; Pociot, F.; Gornik, O. Altered IgG N-Glycosylation at Onset of Type 1 Diabetes in Children Is Predominantly Driven by Changes in the Fab N-Glycans. *Biomedicines* **2025**, *13* (5), 1206. https://doi.org/10.3390/biomedicines13051206.
(41) Krištić, J.; Lauc, G. The Importance of IgG Glycosylation—What Did We Learn after Analyzing over 100,000 Individuals. *Immunol. Rev.* **2024**, *328* (1), 143–170. https://doi.org/10.1111/imr.13407.
(42) Zhang, Y. Understanding the Impact of Fc Glycosylation on Its Conformational Changes by Molecular Dynamics Simulations and Bioinformatics. *Mol. Biosyst.* **2015**, *11* (12), 3415–3424. https://doi.org/10.1039/C5MB00602C.
(43) Sha, S.; Agarabi, C.; Brorson, K.; Lee, D.-Y.; Yoon, S. N-Glycosylation Design and Control of Therapeutic Monoclonal Antibodies. *Trends Biotechnol.* **2016**, *34* (10), 835–846. https://doi.org/10.1016/j.tibtech.2016.02.013.
(44) Krasnova, L.; Wong, C.-H. Making Universal Vaccines and Antibodies Through Glycoengineering. In *Cancer Vaccines*; Padler-Karavani, V., Ed.; Methods in Molecular Biology; Springer US: New York, NY, 2025; Vol. 2926, pp 35–50. https://doi.org/10.1007/978-1-0716-4542-0_3.

(45) Wang, Q.; Chung, C.; Chough, S.; Betenbaugh, M. J. Antibody Glycoengineering Strategies in Mammalian Cells. *Biotechnol. Bioeng.* **2018**, *115* (6), 1378–1393. https://doi.org/10.1002/bit.26567.
(46) Li, S.; McCraw, A. J.; Gardner, R. A.; Spencer, D. I. R.; Karagiannis, S. N.; Wagner, G. K. Glycoengineering of Therapeutic Antibodies with Small Molecule Inhibitors. *Antibodies* **2021**, *10* (4), 44. https://doi.org/10.3390/antib10040044.
(47) Sakae, Y.; Satoh, T.; Yagi, H.; Yanaka, S.; Yamaguchi, T.; Isoda, Y.; Iida, S.; Okamoto, Y.; Kato, K. Conformational Effects of N-Glycan Core Fucosylation of Immunoglobulin G Fc Region on Its Interaction with Fcγ Receptor IIIa. *Sci. Rep.* **2017**, *7* (1), 13780. https://doi.org/10.1038/s41598-017-13845-8.
(48) Kiyoshi, M.; Tsumoto, K.; Ishii-Watabe, A.; Caaveiro, J. M. M. Glycosylation of IgG-Fc: A Molecular Perspective. *Int. Immunol.* **2017**, *29* (7), 311–317. https://doi.org/10.1093/intimm/dxx038.
(49) Wong, W. K.; Robinson, S. A.; Bujotzek, A.; Georges, G.; Lewis, A. P.; Shi, J.; Snowden, J.; Taddese, B.; Deane, C. M. Ab-Ligity: Identifying Sequence-Dissimilar Antibodies That Bind to the Same Epitope. In *MAbs*; Taylor & Francis, 2021; Vol. 13, p 1873478.
(50) Varki, A.; Cummings, R. D.; Aebi, M.; Packer, N. H.; Seeberger, P. H.; Esko, J. D.; Stanley, P.; Hart, G.; Darvill, A.; Kinoshita, T.; Prestegard, J. J.; Schnaar, R. L.; Freeze, H. H.; Marth, J. D.; Bertozzi, C. R.; Etzler, M. E.; Frank, M.; Vliegenthart, J. F.; Lütteke, T.; Perez, S.; Bolton, E.; Rudd, P.; Paulson, J.; Kanehisa, M.; Toukach, P.; Aoki-Kinoshita, K. F.; Dell, A.; Narimatsu, H.; York, W.; Taniguchi, N.; Kornfeld, S. Symbol Nomenclature for Graphical Representations of Glycans. *Glycobiology* **2015**, *25* (12), 1323–1324. https://doi.org/10.1093/glycob/cwv091.
(51) Webb, B.; Sali, A. Protein Structure Modeling with MODELLER. In *Functional Genomics*; Kaufmann, M., Klinger, C., Savelsbergh, A., Eds.; Methods in Molecular Biology; Springer New York: New York, NY, 2017; Vol. 1654, pp 39–54. https://doi.org/10.1007/978-1-4939-7231-9_4.
(52) Altschul, S. F.; Gish, W.; Miller, W.; Myers, E. W.; Lipman, D. J. Basic Local Alignment Search Tool. *J. Mol. Biol.* **1990**, *215* (3), 403–410. https://doi.org/10.1016/S0022-2836(05)80360-2.
(53) Zhang, Y.; Skolnick, J. TM-Align: A Protein Structure Alignment Algorithm Based on the TM-Score. *Nucleic Acids Res.* **2005**, *33* (7), 2302–2309.
(54) Kern, N. R.; Lee, J.; Choi, Y. K.; Im, W. CHARMM-GUI Multicomponent Assembler for Modeling and Simulation of Complex Multicomponent Systems. *Nat. Commun.* **2024**, *15* (1), 5459. https://doi.org/10.1038/s41467-024-49700-4.
(55) Kern, J.; Chatterjee, R.; Young, I. D.; Fuller, F. D.; Lassalle, L.; Ibrahim, M.; Gul, S.; Fransson, T.; Brewster, A. S.; Alonso-Mori, R.; Hussein, R.; Zhang, M.; Douthit, L.; de Lichtenberg, C.; Cheah, M. H.; Shevela, D.; Wersig, J.; Seuffert, I.; Sokaras, D.; Pastor, E.; Weninger, C.; Kroll, T.; Sierra, R. G.; Aller, P.; Butryn, A.; Orville, A. M.; Liang, M.; Batyuk, A.; Koglin, J. E.; Carbajo, S.; Boutet, S.; Moriarty, N. W.; Holton, J. M.; Dobbek, H.; Adams, P. D.; Bergmann, U.; Sauter, N. K.; Zouni, A.; Messinger, J.; Yano, J.; Yachandra, V. K. Structures of the Intermediates of Kok's Photosynthetic Water Oxidation Clock. *Nature* **2018**, *563* (7731), 421–425. https://doi.org/10.1038/s41586-018-0681-2.
(56) Berendsen, H. J. C.; Spoel, D.; Drunen, R. GROMACS: A Message-passing Parallel Molecular Dynamics Implementation. *Comput. Phys. Commun.* **1995**, *91*, 43–56. https://doi.org/10.1016/0010-4655(95)00042-E.

(57) de Brevern, A. G.; Etchebest, C.; Hazout, S. Bayesian Probabilistic Approach for Predicting Backbone Structures in Terms of Protein Blocks. *Proteins* **2000**, *41* (3), 271–287. https://doi.org/10.1002/1097-0134(20001115)41:3%253C271::aid-prot10%253E3.0.co;2-z.
(58) Stanfield, R. L.; Zemla, A.; Wilson, I. A.; Rupp, B. Antibody Elbow Angles Are Influenced by Their Light Chain Class. *J. Mol. Biol.* **2006**, *357* (5), 1566–1574. https://doi.org/10.1016/j.jmb.2006.01.023.
(59) Van der Maaten, L.; Hinton, G. Visualizing Data Using T-SNE. *J. Mach. Learn. Res.* **2008**, *9* (11).
(60) Wang, Y.; Huang, H.; Rudin, C.; Shaposhnik, Y. Understanding How Dimension Reduction Tools Work: An Empirical Approach to Deciphering t-SNE, UMAP, TriMAP, and PaCMAP for Data Visualization. *J. Mach. Learn. Res.* **2021**, *22* (201), 1–73.
(61) Kang, P. W.; Westerlund, A. M.; Shi, J.; White, K. M.; Dou, A. K.; Cui, A. H.; Silva, J. R.; Delemotte, L.; Cui, J. Calmodulin Acts as a State-Dependent Switch to Control a Cardiac Potassium Channel Opening. *Sci. Adv.* **2020**, *6* (50), eabd6798. https://doi.org/10.1126/sciadv.abd6798.
(62) Westerlund, A. M.; Fleetwood, O.; Pérez-Conesa, S.; Delemotte, L. Network Analysis Reveals How Lipids and Other Cofactors Influence Membrane Protein Allostery. *J. Chem. Phys.* **2020**, *153* (14), 141103. https://doi.org/10.1063/5.0020974.
(63) Wang, Y.; Lamim Ribeiro, J. M.; Tiwary, P. Machine Learning Approaches for Analyzing and Enhancing Molecular Dynamics Simulations. *Curr. Opin. Struct. Biol.* **2020**, *61*, 139–145. https://doi.org/10.1016/j.sbi.2019.12.016.
(64) Tramontano, A.; Chothia, C.; Lesk, A. M. Framework Residue 71 Is a Major Determinant of the Position and Conformation of the Second Hypervariable Region in the VH Domains of Immunoglobulins. *J. Mol. Biol.* **1990**, *215* (1), 175–182. https://doi.org/10.1016/S0022-2836(05)80102-0.
(65) Foote, J.; Winter, G. Antibody Framework Residues Affecting the Conformation of the Hypervariable Loops. *J. Mol. Biol.* **1992**, *224* (2), 487–499. https://doi.org/10.1016/0022-2836(92)91010-M.
(66) Ma, B. Correlation of N-Glycan Dynamics and Interaction Network with Allosteric Antigen Binding and Fc Receptor Recognition. *Explor. Immunol.* **2021**, *1* (1), 27–36. https://doi.org/10.37349/ei.2021.00004.
(67) Natesan, R.; Agrawal, N. J. IgG1 and IgG4 Antibodies Sample Initial Structure Dependent Local Conformational States and Exhibit Non-Identical Fab Dynamics. *Sci. Rep.* **2023**, *13* (1), 4791. https://doi.org/10.1038/s41598-023-32067-9.
(68) Spiteri, V. A.; Doutch, J.; Rambo, R. P.; Bhatt, J. S.; Gor, J.; Dalby, P. A.; Perkins, S. J. Using Atomistic Solution Scattering Modelling to Elucidate the Role of the Fc Glycans in Human IgG4. *PLOS ONE* **2024**, *19* (4), e0300964. https://doi.org/10.1371/journal.pone.0300964.
(69) Tarenzi, T.; Rigoli, M.; Potestio, R. Communication Pathways Bridge Local and Global Conformations in an IgG4 Antibody. *Sci. Rep.* **2021**, *11* (1), 23197. https://doi.org/10.1038/s41598-021-02323-x.
(70) Subedi, G. P.; Barb, A. W. The Structural Role of Antibody N-Glycosylation in Receptor Interactions. *Structure* **2015**, *23* (9), 1573–1583. https://doi.org/10.1016/j.str.2015.06.015.

(71) Wang, X.; Kumar, S.; Buck, P. M.; Singh, S. K. Impact of Deglycosylation and Thermal Stress on Conformational Stability of a Full Length Murine igG2a Monoclonal Antibody: Observations from Molecular Dynamics Simulations. *Proteins Struct. Funct. Bioinforma.* **2013**, *81* (3), 443–460. https://doi.org/10.1002/prot.24202.
(72) Subedi, G. P.; Barb, A. W. The Structural Role of Antibody N-Glycosylation in Receptor Interactions. *Structure* **2015**, *23* (9), 1573–1583. https://doi.org/10.1016/j.str.2015.06.015. P.; Barb, A. W. The Structural Role of Antibody N-Glycosylation in Receptor Interactions. *Structure* **2015**, *23* (9), 1573–1583. https://doi.org/10.1016/j.str.2015.06.015. .06.015.